WATER RESOURCES RESEARCH, VOL. 29, NO. 8, PAGES 2615–2627, AUGUST 1993

A Quadratic Petrov-Galerkin Solution for Kinematic Wave Overland Flow

RAFAEL MUÑOZ-CARPENA

Department of Biological and Agricultural Engineering, North Carolina State University, Raleigh

CASS T. MILLER

Department of Environmental Sciences and Engineering, University of North Carolina, Chapel Hill

JOHN E. PARSONS

Department of Biological and Agricultural Engineering, North Carolina State University, Raleigh

A Petrov-Galerkin (PG) finite element method was developed to solve the kinematic wave formulation of the overland flow equations. The resultant model uses quadratic basis functions and test functions that are modified by polynomials of cubic and quartic order, yielding a formulation that includes four PH parameters. The PG model was found to reduce the mean sum of square error of the solution compared to a conventional Bubnov-Galerkin finite element solution by about a factor of 3 as the Courant number (Cr) approached one. Good results were also achieved with the PG method for problems that resulted in shock formation, which are typical of many applied problems of concern. PG parameters were found to depend strongly upon the Courant number and weakly upon the number of nodes in the system. Polynomial expressions were derived to approximate the PG parameters over the range $0 < Cr < 1$. As the number of nodes in the system increased, a single-parameter version of the model yielded solutions approaching the accuracy of the four-parameter model.

1. INTRODUCTION

Overland flow routing is the term used to describe the movement of water over a surface and implies the calculation of flow rates at positions along a hillslope at different time steps [*Lane et al.*, 1987]. The movement of surface water can be described by continuity and momentum equations applied to an incompressible fluid (Saint-Venant equations).

An accurate, stable, and efficient solution to the Saint-Venant equations is necessary for several common problems. Originally, these equations were used to describe river and channel routing problems. Since then they have been applied to overland flow, watershed modeling, and runoff determination. Flow solutions of this type are also the foundation upon which sediment transport and nonpoint source pollutant transport models are based.

Since overland flow processes are transient, the description of such processes requires the simultaneous solution of a coupled system of partial differential equations. Simplification of the Saint-Venant equations is appropriate for many common problems. One such simplification is the kinematic wave approximation. Since its formulation by *Lighthill and Whitham* [1955] and its application to watershed modeling by *Henderson and Wooding* [1964] using the method of characteristics (MOC), many researchers have used the kinematic wave approach for runoff and overland flow problems [*Brakensiek*, 1967; *Woolhiser*, 1969; *Eagleson*, 1970; *Li et al.*, 1975; Borah et al., 1980].

Under certain conditions the kinematic wave equations give rise to sharp-front solutions, in which values of the dependent variable change rapidly in space and time over a portion of the domain [*Taylor*, 1976; *Ross et al.*, 1979; *Vieux et al.*, 1990]. These sharp fronts have been termed kinematic shock waves [*Lighthill and Whitham*, 1955; *Kibler and Woolhiser*, 1972; *Li et al.*, 1975; *Singh*, 1975; *Borah et al.*, 1980; *Zhang and Cundy*, 1989]. While the method of characteristics is well suited to the solution of sharp-front problems, the common occurrence of irregularly shaped domains with spatially varying properties has led to the routine application of Eulerian methods for solution of kinematic wave problems. However, Eulerian methods are prone to phase errors, oscillations in the solution, and numerical dispersion when used to approximate such sharp-front problems [*Zienkiewicz*, 1977; *Huyakorn and Pinder*, 1983; *Hromadka and DeVries*, 1988; *Ponce*, 1991]. Recent advances in Petrov-Galerkin (PG) finite element methods (FEMs) have resulted in reductions in such errors compared to conventional Eulerian formulation for advective-dominated transport and multiphase flow and transport problems [*Westerink and Shea*, 1989; *Cornew and Miller*, 1990; *Mayer and Miller*, 1990; *Miller and Cornew*, 1992]. The purpose of this work is to develop and evaluate a PG FEM solution for the kinematic wave equations.

2. BACKGROUND

2.1. *Overland Flow*

Overland flow may be described by the classical Saint-Venant equations, which include a dynamic continuity equation and a dynamic linear momentum equation applied to an incompressible fluid for a one-dimensional system, as [*Bras*, 1990]

$$\frac{\partial h}{\partial t} + \frac{\partial q}{\partial x} = r = i - f \tag{1}$$

Paper number 93WR00610.
0043-1397/93/93WR-00610$05.00

$$\frac{\partial v}{\partial t} + v \frac{\partial v}{\partial x} + g \frac{\partial h}{\partial x} = g(S_0 - S_f) - \frac{vr}{h} \tag{2}$$

where $h(x, t)$ is the vertical flow depth (meters); $q(x, t)$ is the discharge per unit width (square meters per second); r is the rainfall excess, or lateral inflow (meters per second); i is the rainfall intensity (meters per second); f is the infiltration rate (meters per second); v is the depth-averaged velocity (meters per second); g is the gravitational constant (m/s^2); S_0 is the bed slope; S_f is the friction slope; x is the direction of flow (meters); and $q = vh$.

Depending on the case studied, several implications of the momentum equation, equation (2), are possible [*Bedient and Huber*, 1988]. The kinematic wave equations result from the assumption that the hydrodynamic terms of the momentum equation are negligible, which is reasonable for the case where no backwater exists [*Lighthill and Whitham*, 1955]. In this case, the momentum equation becomes $S_f = S_0$.

A constitutive relation is needed to express the discharge, q, as a function of h. Manning's equation is often used for this relation:

$$q(h) = \frac{(S_0)^{1/2}}{n} h^{5/3} \tag{3}$$

where n is Manning's roughness coefficient.

The numerical solution to the kinematic wave equations can be characterized in terms of three dimensionless parameters [*Lighthill and Whitham*, 1955; *Henderson*, 1966; *Woolhiser and Liggett*, 1967]:

$$Fr = \frac{v}{(gh)^{1/2}} \tag{4}$$

$$k = \frac{LS_0 g}{v^2} \tag{5}$$

$$Cr = \frac{c\Delta t}{\Delta x} \tag{6}$$

for

$$c = \frac{\partial q}{\partial h} = \frac{5(S_0)^{1/2}}{3n} h^{2/3} \tag{7}$$

where Fr is the Froude number, k is the kinematic flow number, Cr is the Courant number, Δt is the temporal grid spacing, Δx is the spatial grid spacing, and c is the celerity of the kinematic wave [*Lighthill and Whitham*, 1955; *Bras*, 1990].

The Fr is a ratio of inertial to gravitational forces. For normal floods in natural rivers, or overland flow processes, dynamic wave fronts attenuate very rapidly as long as $Fr <$ 1.5, and kinematic waves dominate the flood response. A kinematic wave does not dissipate, but it changes in shape (steepens) due to the dependency of the velocity on the depth. If the steepening process stops, the result is a monoclinal steady state wave [*Henderson*, 1966].

A restriction on the kinematic number of $k > 10$ ensures that the kinematic wave assumptions introduce less than a 10% error in the solution [*Woolhiser and Liggett*, 1967]. Only for very flat ($S_0 < 0.002$) or very steep ($S_0 > 0.10$) slopes is the kinematic assumption violated.

The Cr is a measure of the temporal discretization relative to the spatial discretization and the characteristic wave velocity of the system. The Cr affects the stability and accuracy of the solution in the explicit case and accuracy of the solution for the implicit case [*Vieux and Segerlind*, 1989; *Blandford and Meadows*, 1990; *Mohtar et al.*, 1990]. A stability criterion for the explicit case requires $Cr < 1$, while solution accuracy improves as the Cr decreases to 0.2 [*Viessman et al.*, 1977]. Implicit formulations are unconditionally stable, but the accuracy of solution improves as Cr decreases [*Blandford and Meadows*, 1990; *Vieux et al.*, 1990].

Two additional parameters of interest for case of steady rainfall over an impermeable plane are

$$q_m = rL \tag{8}$$

$$t_e = \left(\frac{L}{\alpha r^{2/3}} \right)^{3/5} \tag{9}$$

where L is the length of the domain, q_m is the maximum discharge, t_e is the time to equilibrium for a point a distance L away from the boundary, and α is the leading coefficient from Manning's equation, which may be defined as

$$\alpha = \frac{(S_0)^{1/2}}{n} \tag{10}$$

The initial and boundary conditions considered herein can be described as

$$h(t = 0,\ 0 \le x \le L) = 0 \tag{11}$$

$$h(t > 0,\ 0) = h_0 \tag{12}$$

Note that the boundary condition can be modified for different cases. One case could be when no upslope inflow occurs ($h_0 = 0$) for a general overland flow problem, where $x = 0$ is the beginning of the slope. A second case could be a constant upslope inflow ($h(t, x = 0) > 0$). A more realistic case is a boundary condition where $h(t, x = 0) = h_0(t)$, depending on the inflow hydrograph from an adjacent field upslope. Eulerian methods accommodate such changes in auxiliary conditions easily.

The rainfall excess, r, is the rainfall rate less the infiltration rate, which may be expected to vary in space and time for typical field conditions. The infiltration rate can be handled using any of the approximate methods available such as Green-Ampt, Philip, Holtan and Horton [*Skaggs et al.*, 1969] or a more exact method based on a solution to Richards's equation [*Richards*, 1931]. *Schmid* [1989] investigated the implicit assumption in the model that infiltration is independent of overland flow so that only the weak coupling of both processs is taken into account. He found that the errors introduced were in most cases smaller than 5% and always less than 11%. Compared to the uncertainty introduced by spatial variability in subsurface conditions, the weak coupling assumption seems appropriate.

2.2. *Solution Methods*

Solutions of kinematic wave equation problems have been formulated and applied for almost 40 years. Characteristic, finite difference, finite element, and control volume finite element methods have been used in these solution schemes.

A detailed description of each of these solutions is beyond the scope of this work. However, several results of solutions in the literature pertain to the development of new methods.

For domains in which model parameters are not spatially variable, the method of characteristics (MOC) is an appropriate solution approach [*Izzard*, 1946; *Lighthill and Whitham*, 1955; *Henderson and Wooding*, 1964; *Wooding*, 1965; *Crawford and Linsley*, 1966; *Woolhiser and Liggett*, 1967]. The success of the MOC is not surprising. The kinematic wave equation is a hyperbolic partial differential equation, a class of problem for which the MOC is well suited. Others have extended the MOC to irregularly shaped domains and temporally variable model parameters [*Eagleson*, 1970; *Harley et al.*, 1970; *Singh*, 1976; *Woolhiser*, 1975; *Sherman and Singh*, 1976; *Borah et al.*, 1980; *Parlange et al.*, 1981; *Cundy and Tento*, 1985; *Eggert*, 1987; *Woods and Ibbitt*, 1988; *Sander et al.*, 1990].

While MOC solutions are theoretically attractive, practical problems associated with extension to field conditions have inhibited the widespread use of the MOC [*Ross*, 1977; *Zhang and Cundy*, 1989; *Sander et al.*, 1990]. Surface slope (S_0), roughness (n), and rainfall excess (r) are parameters that vary in space. When such changes are abrupt, discontinuities in h, or kinematic shocks, result [*Kibler and Woolhiser*, 1972]. While such problems can be solved using the MOC [*Borah et al.*, 1980; *Hunt*, 1987], a more common approach has been to use Eulerian methods, i.e., finite differences [*Stoker*, 1953; *Brakensiek*, 1967; *Liggett and Woolhiser*, 1967; *Amein*, 1968; *Amein and Fang*, 1970; *Kibler and Woolhiser*, 1972; *Price*, 1974; *Li et al.*, 1975; *Zhang and Cundy*, 1989], finite elements [*Judah*, 1972; *Ross et al.*, 1979; *Vieux and Segerlind*, 1989; *Blandford and Meadows*, 1990; *Vieux et al.*, 1990; *Goodrich et al.*, 1991], mixed formulations (MOC and finite differences) [*Singh*, 1975], or a control volume scheme [*Mohtar et al.*, 1990].

While Eulerian methods allow for the simple incorporation of spatially variable parameters, they are not well suited to the solution of hyperbolic equations. Recent work has suggested using Eulerian solution methods with refined spatial and temporal discretization and smoothed values of spatially variable parameters to avoid numerical errors associated with kinematic shocks [*Ponce*, 1991; *Vieux et al.*, 1990].

Upstream weighting methods have been used to reduce errors associated with the application of Eulerian methods to sharp-front problems [*Hughes*, 1978; *Heinrich and Zienkiewicz*, 1977; *Wait and Mitchell*, 1985]. In particular, recent advances have been made in applying PG methods to solve advective-dominated transport problems [*Westerink and Shea*, 1989; *Cantekin and Westerink*, 1990; *Cornew and Miller*, 1990; *Miller and Cornew*, 1992] and multiphase flow and transport problems [*Mayer and Miller*, 1990]. The success of these applications suggests that similar methods may be applicable to kinematic wave problems.

3. Solution Formulation

Based upon results achieved for other sharp-front problems [*Westerink and Shea*, 1989; *Cantekin and Westerink*, 1990; *Cornew and Miller*, 1990; *Mayer and Miller*, 1990] a PG approach may be formulated to solve the kinematic wave equations. The formulation is a straightforward extension of methods that have been developed and applied successfully to problems that pose many of the same numerical difficulties as the kinematic wave equations. However, evaluating the improvements offered by such a method, determining optimal parameters for the approach, and testing the approach on shock-type problems are not trivial and are necessary to advance the understanding of such Eulerian strategies for solving kinematic wave problems.

Equation (1) may be written in a weak weighted residual form as

$$\int_{\mathfrak{D}} W_i\left(\frac{\partial \hat{h}}{\partial t}+\frac{\partial \hat{q}}{\partial x}-r\right) dx = 0 \qquad i = 1, \cdots, n_n \tag{13}$$

for trial solutions described over an element of the form

$$\hat{h}(x) = \sum_{j=1}^{n_{ne}} N_j(x)h_j \tag{14}$$

$$\hat{q}(x) = \sum_{j=1}^{n_{ne}} N_j(x)q_j = \sum_{j=1}^{n_{ne}} \alpha(x)N_j(x)h_j^{5/3} \tag{15}$$

where W_i is a weighting, or test, function corresponding to node i; N_j are standard Lagrange polynomial basis functions; n_n is the number of nodes in the domain, $\mathfrak{D}$; and n_{ne} is the number of nodes in an element. Resolving the time derivative using a variably weighted finite difference approximation gives

$$\int_{\mathfrak{D}} W_I\left[\hat{h}^{l+1} + \theta\Delta t\left(\frac{\partial \hat{q}^{l+1}}{\partial x} - r^{l+1}\right)\right] dx = \int_{\mathfrak{D}} W_I\left[\hat{h}^{l} - (1-\theta)\Delta t\left(\frac{\partial \hat{q}^{l}}{\partial x} - r^{l}\right)\right] dx \tag{16}$$

where l is a time step index; θ is a time-weighting coefficient, which is equal to 0.5 for Crank-Nicolson weighting; and the captial subscript, I, on W is used to denote a system of equations (one equation for each of the nodes in the domain).

The basis functions may be specified as quadratic Lagrange polynomials in natural coordinates ($-1 \le \xi \le 1$) for every element by

$$N_j(\xi) = \prod_{\substack{n=1\\ n\neq j}}^{3} \frac{(\xi - \xi_n)}{(\xi_j - \xi_n)} \tag{17}$$

which yields piecewise continuous basis functions of the usual form [*Zienkiewicz*, 1977].

The weighting functions are modified by cubic (M_3) and quartic (M_4) functions giving [*Westerink and Shea*, 1989]

$$W_1(\xi) = N_1(\xi) - \alpha_c M_3(\xi) - \beta_c M_4(\xi) \tag{18}$$

$$W_2(\xi) = N_2(\xi) + 4\alpha_m M_3(\xi) + 4\beta_m M_4(\xi) \tag{19}$$

$$W_3(\xi) = N_3(\xi) - \alpha_c M_3(\xi) - \beta_c M_4(\xi) \tag{20}$$

for

$$M_3(\xi) = \frac{5}{8}\,\xi(\xi+1)(\xi-1) \tag{21}$$

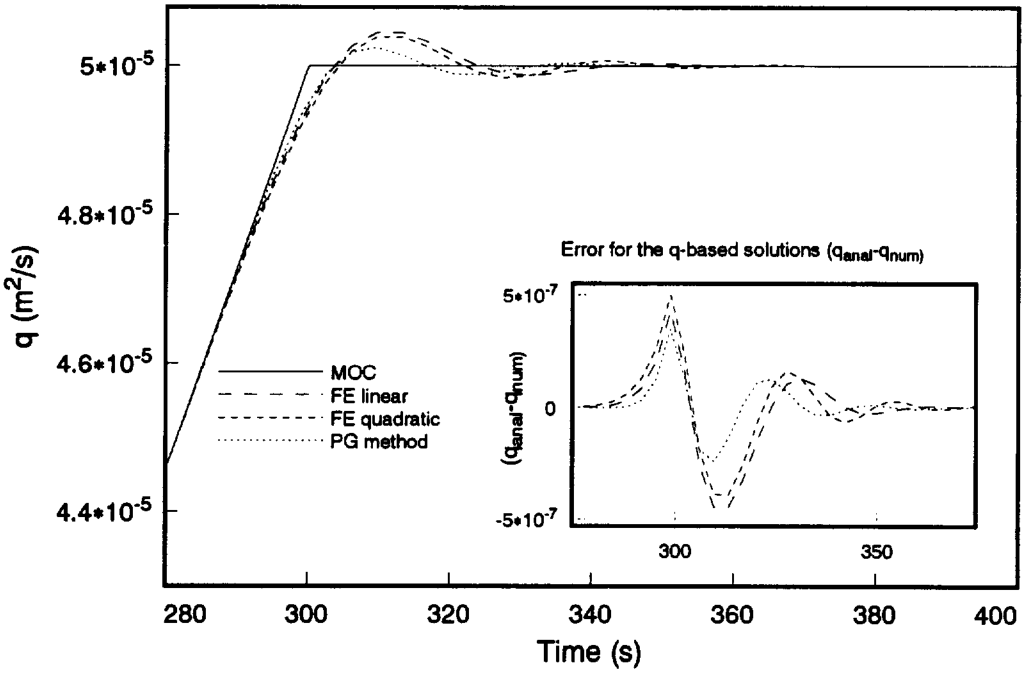

Fig. 1. Comparison of q-based solutions to the kinematic wave equation for the case of a constant rainfall over an impermeable plane.

$$M_4(\xi) = -\frac{21}{16}(\xi^4 - \xi^2) \tag{22}$$

The constants α_c, β_c, α_m, and β_m are PG parameters required to specify the form of the weighting functions for the corner element ($\xi = \pm 1$) and midelement ($\xi = 0$) nodes, respectively.

The PG finite element solution yields a system of linear equations of the form

$$[A]\{h\}^{l+1,m+1} = \{b\} = \{b_l\}^l + \{b_n\}^{l+1,m} \tag{23}$$

where m is the iteration level of the solution, $[A]$ is a banded coefficient matrix that contains only linear terms, $\{b\}$ is a vector that contains all terms evaluated at the l time level and the $\hat{q}$ term evaluated at the new time level but lagged an iteration level, $\{b_l\}^l$ is the linear portion of $\{b\}$, and $\{b_n\}^{l+1,m}$ is the nonlinear portion of $\{b\}$.

The global matrix $[A]$ and vectors $\{b_l\}^l$ and $\{b_n\}^{l+1,m}$

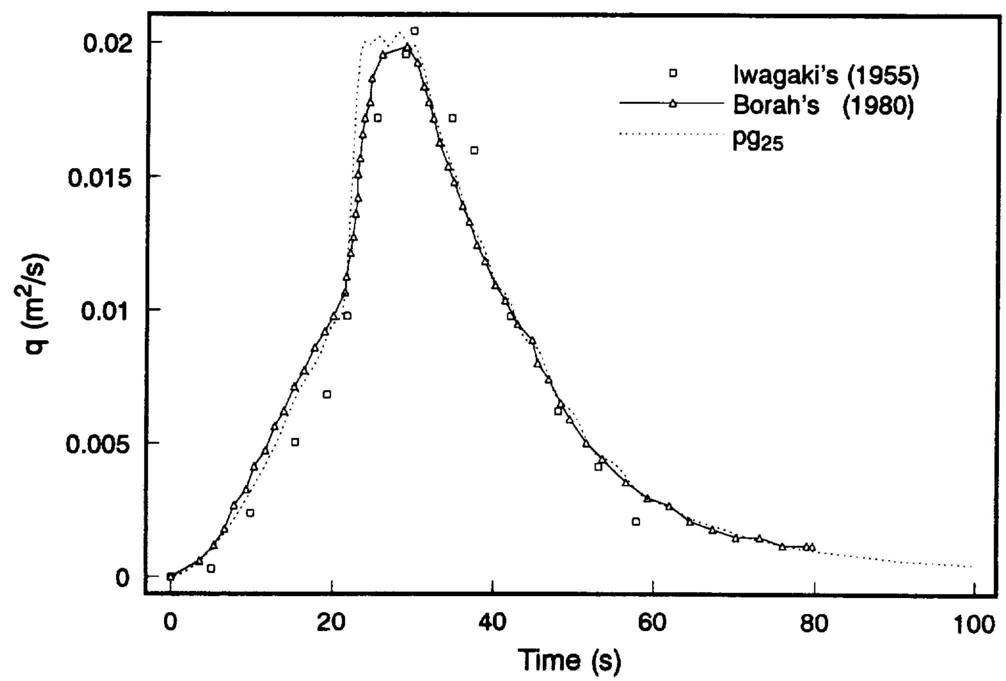

Fig. 2. Comparison of model simulation results and experimental data [*Iwagaki*, 1955] for a three-slope domain (Table 1, case 2).

TABLE 1. Summary of Simulation Parameters

Case	Section	L, m	r, m/s	t_r, s	n	S_0	n_n	Δx, m	Δt, s	Cr	Fr	k
1	···	15.0	3.33×10^{-6}	t_s	0.048	0.0576	51	0.3	3.60	1.00	0.505	3390.
2	1	8.0	1.08×10^{-3}	30	0.009	0.0200	9	1.0	0.42	0.55	2.37	2.58
	2	8.0	6.38×10^{-4}	30	0.009	0.0150	8	1.0	0.42	0.60	2.18	3.17
	3	8.0	8.00×10^{-4}	30	0.009	0.0100	8	1.0	0.42	0.62	1.89	2.98
3	1	7.5	3.33×10^{-6}	1500	0.048	0.0576	26	0.3	3.60	0.76	0.471	2950.
	2	7.5	3.33×10^{-6}	1500	0.100	0.0576	25	0.3	3.60	0.64	0.261	8180.
4	1	5.0	3.33×10^{-6}	1500	0.100	0.0400	17	0.31	6.24	0.74	0.198	5680.
	2	5.0	3.33×10^{-6}	1500	0.100	0.0100	16	0.31	6.24	0.56	0.114	3740.
	3	5.0	3.33×10^{-6}	1500	0.100	0.0025	16	0.31	6.24	0.44	0.064	2330.
5	···	10–50	1.00×10^{-6}	t_s	0.006–0.007	0.01–0.02	11–201	0.25–1.0	0.07–9.9	0.05–1.00	1.50	500.
6	···	25.0	1.00×10^{-6}	t_s	0.00647	0.0137	51	0.5	0.18–3.7	0.05–1.00	1.50	500.

Here t_r is the duration of rainfall, and t_s is the time simulated.

result from the summation of elemental contributions of the form

$$[A] = \sum_{n_e=1}^{ne} [A_e^{n_e}] \tag{24}$$

$$\{b_l\}^l = \sum_{n_e=1}^{ne} \{b_{el}^{n_e}\}^l \tag{25}$$

$$\{b_n\}^{l+1,m} = \sum_{n_e=1}^{ne} \{b_{en}^{n_e}\}^{l+1,m} \tag{26}$$

where

$$[A_e^{n_e}] = \frac{\Delta x_{n_e}}{2} \cdot \begin{bmatrix} \int_{-1}^{1} W_1N_1\,d\xi & \int_{-1}^{1} W_1N_2\,d\xi & \int_{-1}^{1} W_1N_3\,d\xi \\ \int_{-1}^{1} W_2N_1\,d\xi & \int_{-1}^{1} W_2N_2\,d\xi & \int_{-1}^{1} W_2N_3\,d\xi \\ \int_{-1}^{1} W_3N_1\,d\xi & \int_{-1}^{1} W_3N_2\,d\xi & \int_{-1}^{1} W_3N_3\,d\xi \end{bmatrix} \tag{27}$$

$$\{b_{el}^{n_e}\}^l = \frac{\Delta x_{n_e}}{2} \cdot \begin{Bmatrix} \int_{-1}^{1} W_1\left\{\hat{h}^l + \Delta t\left[(1-\theta)\left(r^l - \frac{2}{\Delta x_{n_e}}\frac{\partial \hat{q}^l}{\partial \xi}\right) + \theta r^{l+1}\right]\right\} d\xi \\ \int_{-1}^{1} W_2\left\{\hat{h}^l + \Delta t\left[(1-\theta)\left(r^l - \frac{2}{\Delta x_{n_e}}\frac{\partial \hat{q}^l}{\partial \xi}\right) + \theta r^{l+1}\right]\right\} d\xi \\ \int_{-1}^{1} W_3\left\{\hat{h}^l + \Delta t\left[(1-\theta)\left(r^l - \frac{2}{\Delta x_{n_e}}\frac{\partial \hat{q}^l}{\partial \xi}\right) + \theta r^{l+1}\right]\right\} d\xi \end{Bmatrix} \tag{28}$$

$$\{b_{en}^{n_e}\}^{l+1,m} = -\theta\Delta t \begin{Bmatrix} \int_{-1}^{1} W_1 \frac{\partial \hat{q}^{l+1,m}}{\partial \xi}\,d\xi \\ \int_{-1}^{1} W_2 \frac{\partial \hat{q}^{l+1,m}}{\partial \xi}\,d\xi \\ \int_{-1}^{1} W_3 \frac{\partial \hat{q}^{l+1,m}}{\partial \xi}\,d\xi \end{Bmatrix} \tag{29}$$

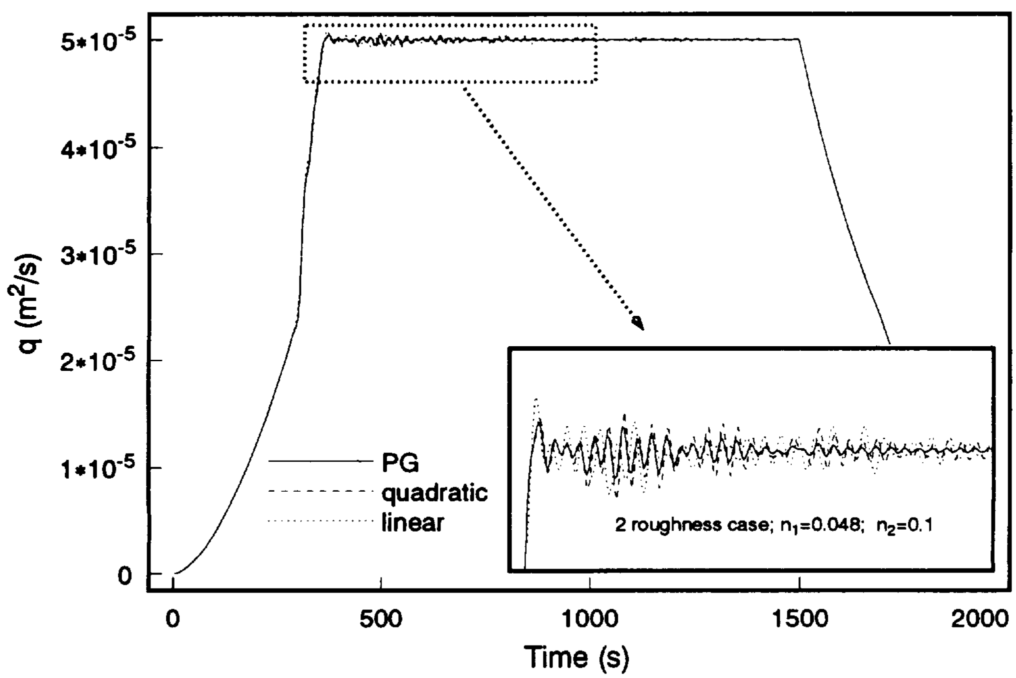

Fig. 3. Comparison of q-based solutions for a two-roughness coefficient domain and a limited duration rainfall (Table 1, case 3).

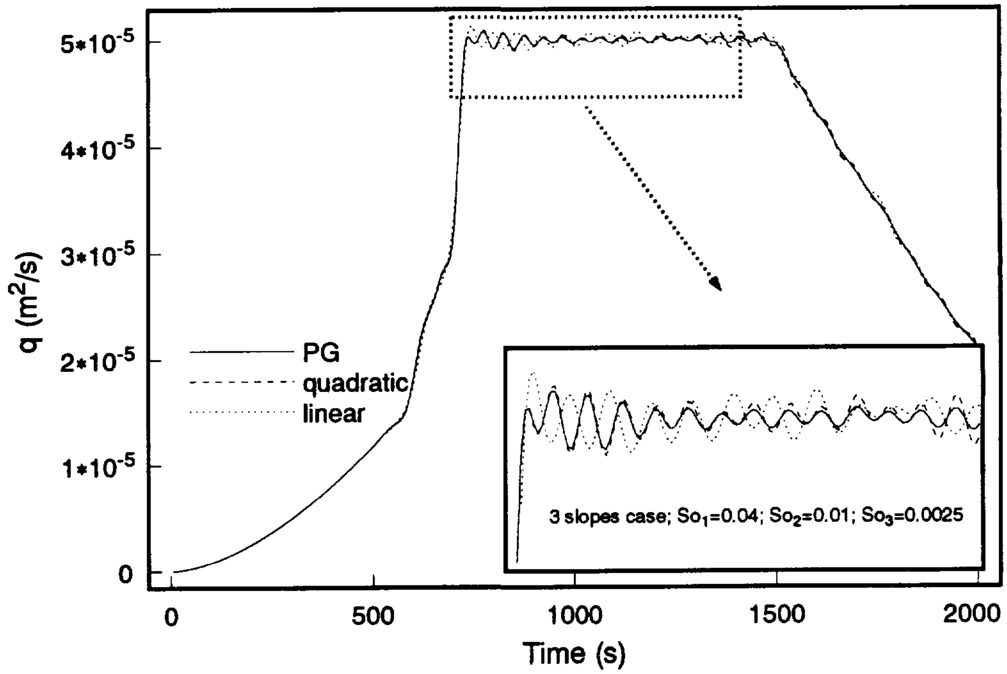

Fig. 4. Comparison of q-based solutions for a three-slope domain and a limited duration rainfall (Table 1, case 4).

n_e is an element index, and ne is the number of elements in the domain.

For a given time step solution, $l + 1$, (23) was solved using Picard iteration and a direct banded solver [*Allen et al.*, 1988] until

$$\frac{\max |h_j^{l+1,m+1} - h_j^{l+1,m}|}{\max |h_j^{l+1,m+1}|} < \varepsilon \qquad (30)$$

where the error tolerance, ε, was set equal to 10^{-10} in this study.

4. Solution Validation

Kinematic wave solutions were solved in two forms: (1) the depth of flow ($h = h(t, x)$) over the surface at each time step, or h based; and (2) the outflow at the end of the domain for each time step ($q = q(t, x = L)$), or q based, which describes a hydrograph. Both of these forms of the solution are useful for a variety of applications.

As a check of the accuracy of the PG solution, a simplified case was considered first. In this case a constant r, S_0, and n exist for a period of time sufficient to build an equilibrium profile over the surface. For these simplified conditions, an analytical solution can be derived by integrating the steady state form of (1), after substituting Manning's equation for q, which gives [*Henderson and Wooding*, 1964; *Woolhiser*, 1975]

TABLE 2. Summary of Errors for Case 4

Error	PG FEM	QBG FEM	LBG FEM
MSE-q	1.13×10^{-13}	1.74×10^{-13}	1.95×10^{-13}
ME	3.31×10^{-6}	3.31×10^{-6}	3.63×10^{-6}
MAE	1.92×10^{-7}	2.63×10^{-7}	2.64×10^{-7}

QBG, quadratic Bubnov Galerkin; LBG, linear Bubnov Galerkin.

$$\begin{aligned} q &= \alpha(rt)^{5/3} && 0 < t < t_e \\ q &= q_m && t \geq t_e \end{aligned} \qquad (31)$$

For the h-based form, an analytical solution based on the method of characteristics [*Henderson and Wooding*, 1964] is

$$h = \min\left[\left(\frac{rx}{\alpha}\right)^{3/5}, rt\right] \qquad t \geq 0 \qquad (32)$$

Model validation was performed using physical and model parameters summarized in Table 1 as case 1 conditions. Figure 1 shows results of the standard Bubnov-Galerkin linear and quadratic finite element solutions; a PG finite element solution, using optimal parameters described below; and the MOC analytical solution, along with the errors associated with the approximate solutions compared to the analytical solution. These graphs illustrate that the PG method reduces the amplitude of the oscillations compared to Bubnov-Galerkin solutions.

A complex shock-producing case was studied by *Iwagaki* [1955]. Runoff was measured from a three-plane cascade, which was made out of a three-section metal flume, with characteristics summarized in Table 1 as case 2 conditions. Over each section of the flume, a different rainfall rate was applied and then stopped at 10, 20, and 30 s in three separate experiments. *Borah et al.* [1980] proposed a kinematic wave shock-fitting model (MOC) to simulate this case. The 30-s rainfall problem was simulated using the Petrov-Galerkin model, with inputs summarized in Table 1 as case 2 conditions. The results shown in Figure 2 illustrate a good agreement among the experimental data, the *Borah et al.* [1980] shock-fitting model, and the PG model developed in this work. *Borah et al.* [1980] note that a standard finite difference method tends to smooth such shocks. The PG method performs well in this case, depicting a shock in the solution comparable to the MOC, with only minimal oscillations even for a relatively coarse discretization (25 nodes). It should be

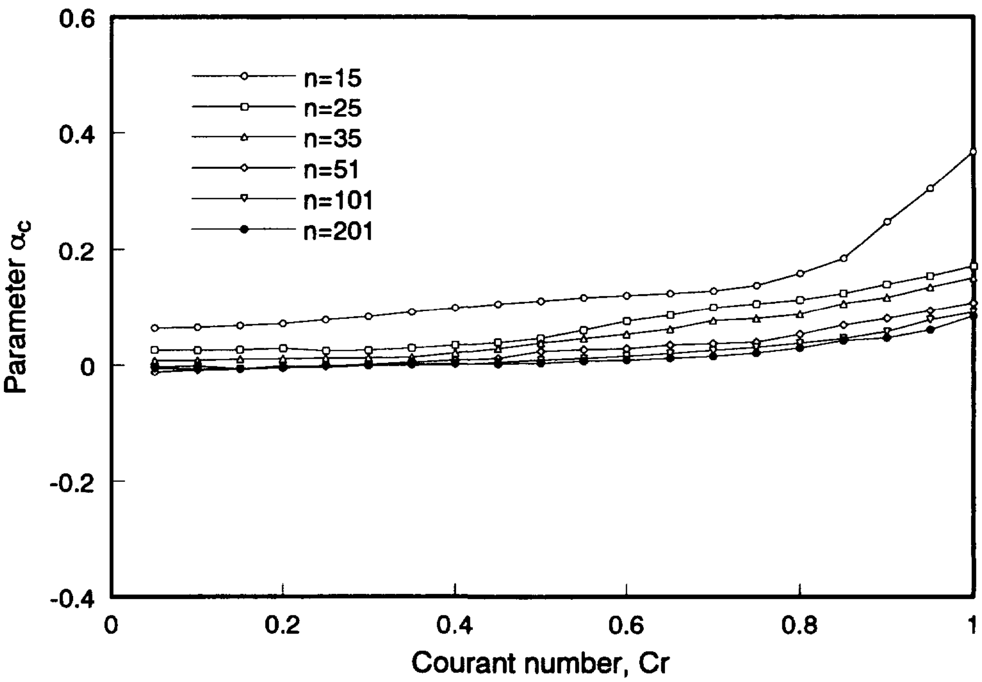

Fig. 5. Optimal values of α_c for the PG method.

noted that some variation is expected between the experimental data and kinematic wave solutions, since $Fr > 1.5$ and $k < 10$.

An additional check was performed for the case of a plane with two equal sections with different Manning's roughnesses and a constant rainfall, stopping at 1500 s to produce a recession hydrograph (case 3 in Table 1). A shock is formed at the change of roughness point (7.5 m). This translates into a change of slope in the hydrograph. Figure 3 shows a comparison between all three FEMs studied (linear, quadratic, and Petrov-Galerkin). A similar simulation was set up for a three-plane cascade with a uniform roughness and all the other parameters the same as in the previous case (case 4 in Table 1). Figure 4 shows the shock in the rising hydrograph caused by the three-slope case. The PG method reduced the amplitude and duration of the errors compared to the linear and quadratic FEM solutions, though all methods perform reasonably well. The solutions were compared with a finely discretized solution (10,000 nodes) to determine errors associated with each method (Table 2).

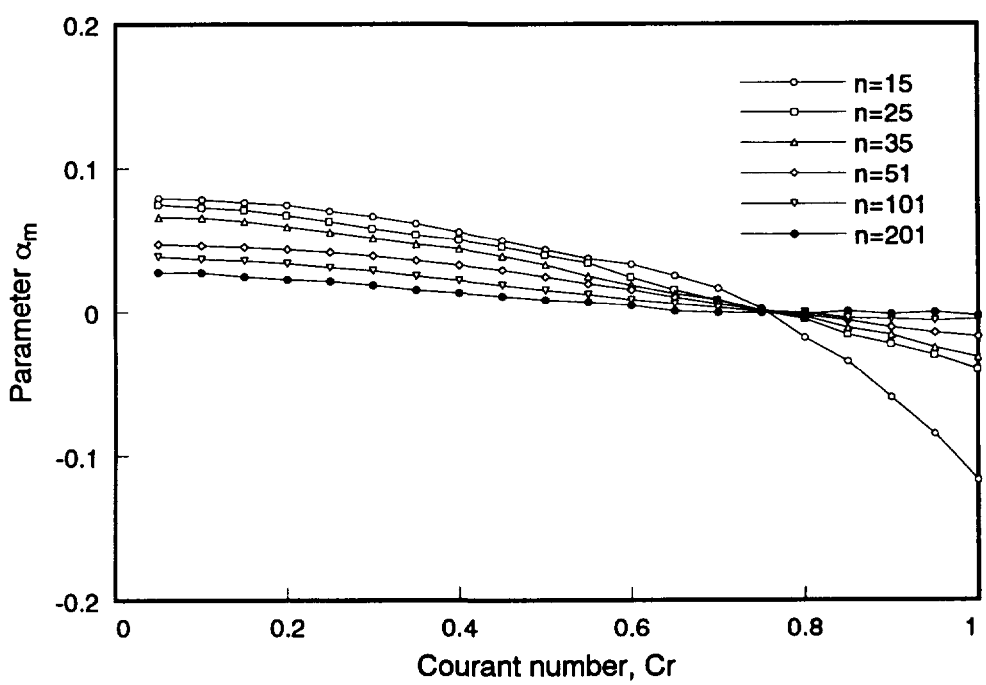

Fig. 6. Optimal values of α_m for the PG method.

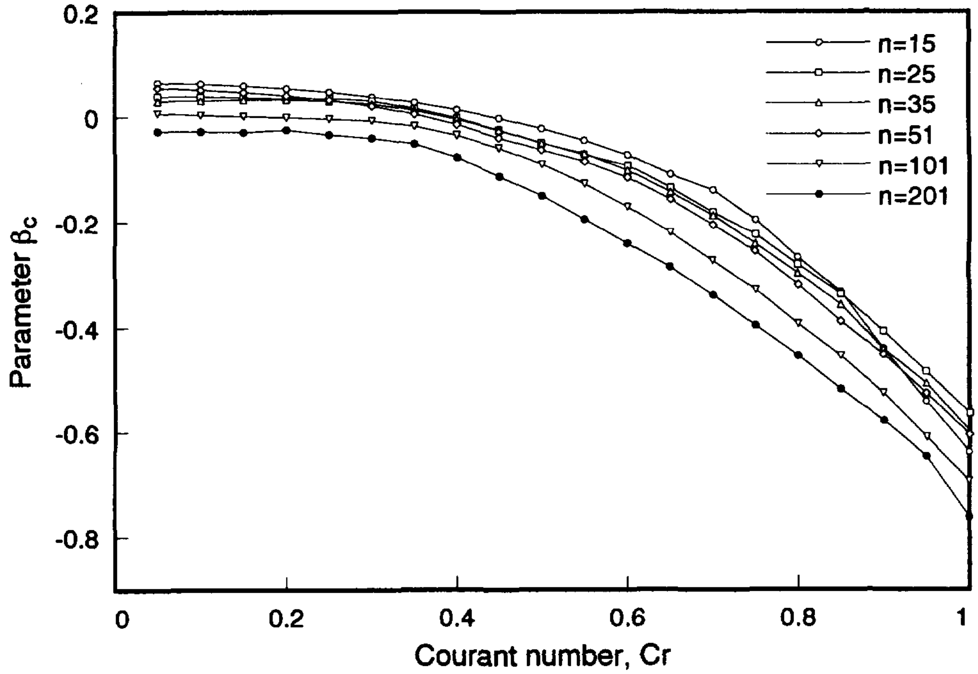

Fig. 7. Optimal values of β_c for the PG method.

Four measures of q- and h-based error were used to judge solution accuracy in this work: mean square error for the h-based solution

$$\text{MSE-}h = \frac{\sum_{l=1}^{n_t} \sum_{j=1}^{n_n} (h_{fj}^l - h_{cj}^l)^2}{n_t n_n} \tag{33}$$

mean square error for the q-based solution

$$\text{MSE-}q = \frac{\sum_{l=1}^{n_t} (q_f^l - q_c^l)^2}{n_t} \tag{34}$$

maximum error

$$\text{ME} = \max |q_f^l - q_c^l| \qquad l = 1, \cdots, n_t \tag{35}$$

and mean absolute error

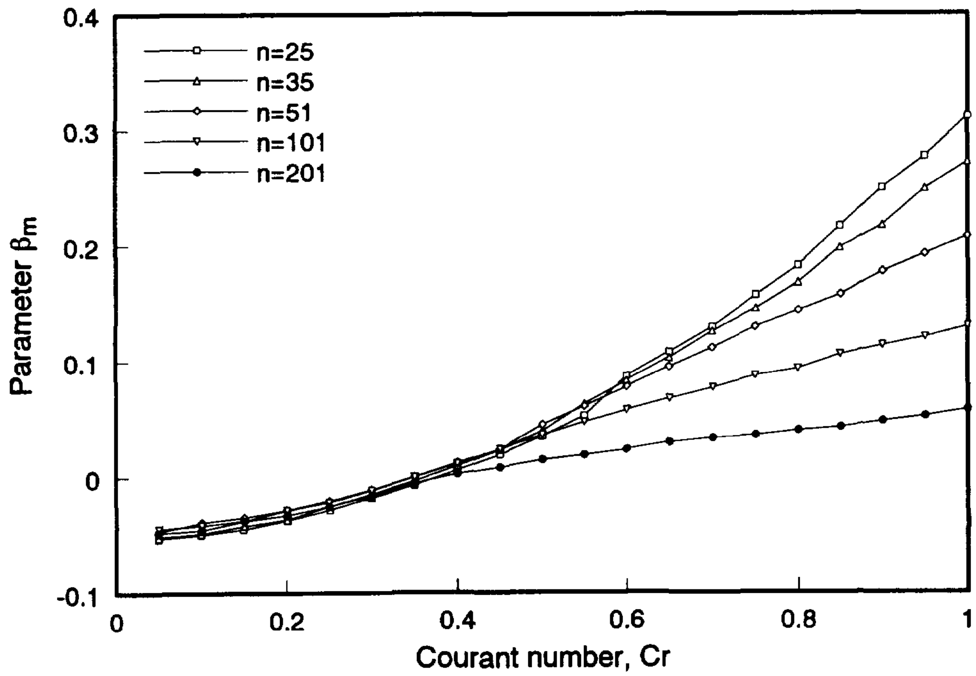

Fig. 8. Optimal values of β_m for the PG method.

TABLE 3. Least Squares Fits of Petrov-Galerkin Parameters

Parameter	a_0	a_1	a_2	a_3	r^2
α_c	−0.00863106	0.0710183	−0.205402	0.223070	0.989
α_m	0.0302084	−0.0225457	−0.0722190	0.0637837	0.992
β_c	−0.0486437	0.369278	−1.22373	0.160394	0.999
β_m	−0.0616601	0.174084	−0.0489402	0.00902134	0.994

Here PG parameter equals $\Sigma_{k=0}^{3} a_k x^k$.

$$\mathrm{MAE} = \frac{\sum_{l=1}^{n_t} |q_f^l - q_c^l|}{n_t} \quad (36)$$

where n_t is the number of time steps, the subscript f denotes the fine-grid (n_n = 10,000) approximation, and the subscript c denotes a coarse-grid approximation.

The validations presented in this section used optimal PG parameters (α_c, α_m, β_c, β_m). Methods used to determine these optimal parameters, the resulting parameter values, and implications for trends in the optimal values are discussed in the following sections.

5. PARAMETER ESTIMATION

An important problem associated with application of the PG method is determination of the PG parameters (α_c, α_m, β_c, β_m) as a function of relevant system parameters. Truncation error analysis, Fourier analysis, and numerical minimization procedures are typically used [*Westerink and Shea*, 1989]. Each method has advantages and disadvantages, but minimization procedures, sometimes called numerical experimentation, have the advantage of acting more directly on the quantity of concern: the difference between a model prediction and the true solution. Truncation analysis usually concentrates on the elimination of low-order truncation error, assuming that the importance of error terms decreases as order increases. Recently, *Miller and Cornew* [1992] found a significant nonmonotonic error contribution from increasing order terms for an advective-dominated transport problem. Fourier analysis methods can yield insight into a problem in terms of errors related to frequencies of a solution, but these have not generally been used to quantitatively predict PG parameters [*Westerink and Shea*, 1989; *Cornew and Miller*, 1990; *Miller and Cornew*, 1992].

A minimization on an h-based PG solution was performed using

$$\min_{\alpha_c, \beta_c, \alpha_m, \beta_m} \sum_{l=1}^{n_t} \sum_{j=1}^{n_n} (h_{aj}^l - h_{mj}^l)^2 \quad (37)$$

where h_a is the analytical solution for depth as a function of space and time, and h_m is the PG model solution for depth as a function of space and time.

The optimization problem described by (37) was solved using a Levenberg-Marquardt method (LMDIF) from the MINPACK mathematical libraries [*Garbow et al.*, 1980] on a Convex C240 supercomputer. The minimization procedure was solved repeatedly for varying values of Cr, Fr, and k. The validity of the results was verified by selecting different starting conditions of the parameters sought and by performing a grid search analysis to inspect the error surface. LMDIF proved to be a robust and reliable estimator of the

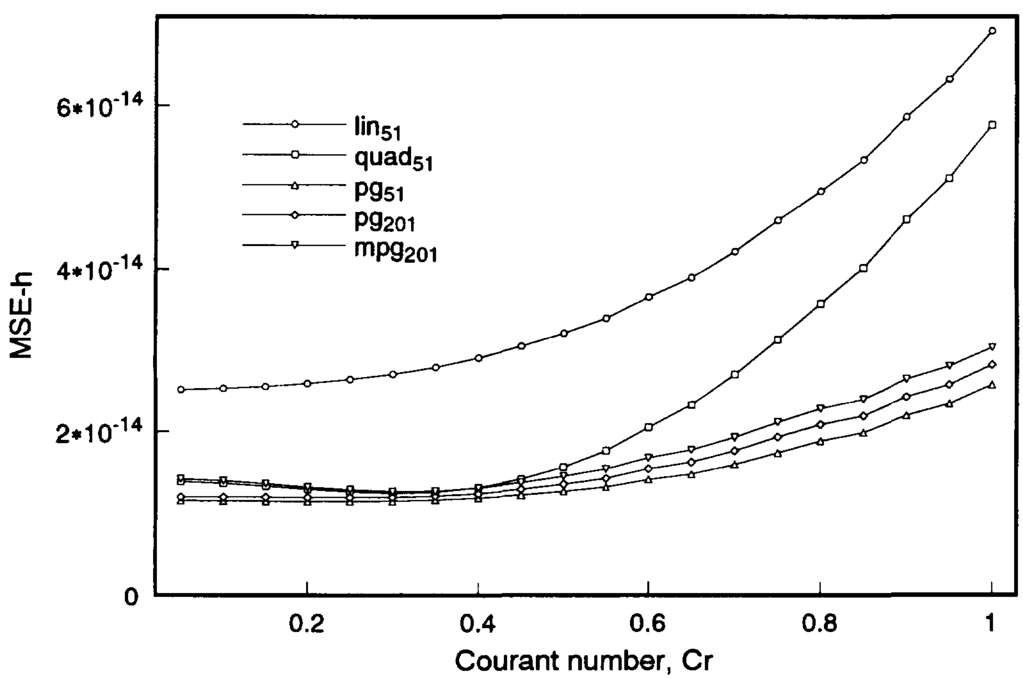

Fig. 9. MSE-h as a function of model formulation, described in Table 4 (Table 1, case 6).

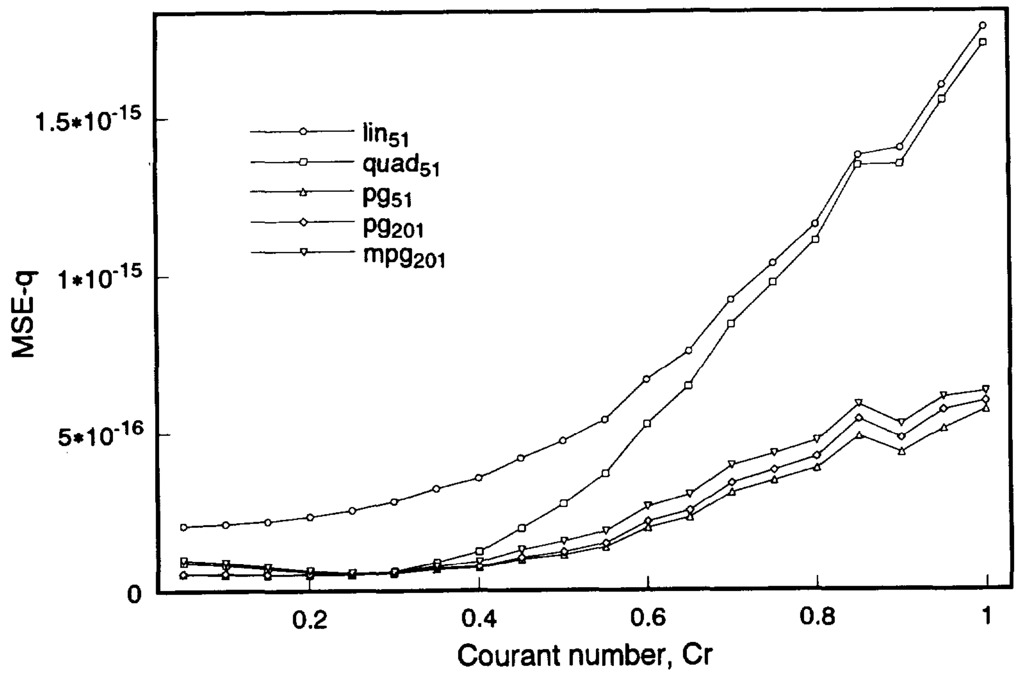

Fig. 10. MSE-q as a function of model formulation, described in Table 4 (Table 1, case 6).

PG parameters that minimized the objective function, equation (37).

Results from the minimization procedure showed that the PG parameters were not only a function of the Cr, but also of the number of nodes in the domain (n_n). However, the parameters were independent of Fr and k. That is, identical optimal PG parameters were determined for a given Cr regardless of the Fr and the k. Upon confirming this finding by an extensive grid search, optimizations were performed for $0.05 \leq Cr \leq 1.00$ in increments of 0.05 and $11 \leq n_n \leq 201$ (Table 1, case 5). This process yielded 200 sets of optimal PG parameters as a sole function of Cr and n_n. Figures 5–8 summarize optimal values from this parameter estimation, while least squares regression of each PG parameter value (for the 201 node case) against Cr yielded the results given in Table 3.

6. Discussion

As the number of nodes increases, optimal values of the PG parameters shown in Figures 5–8 become insensitive to

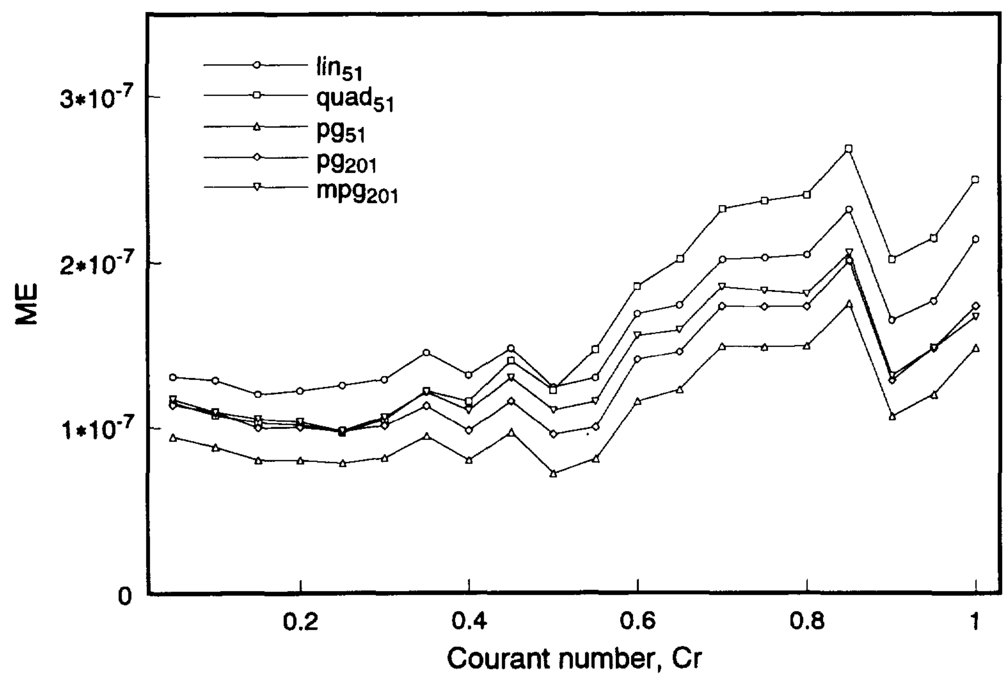

Fig. 11. ME as a function of model formulation, described in Table 4 (Table 1, case 6).

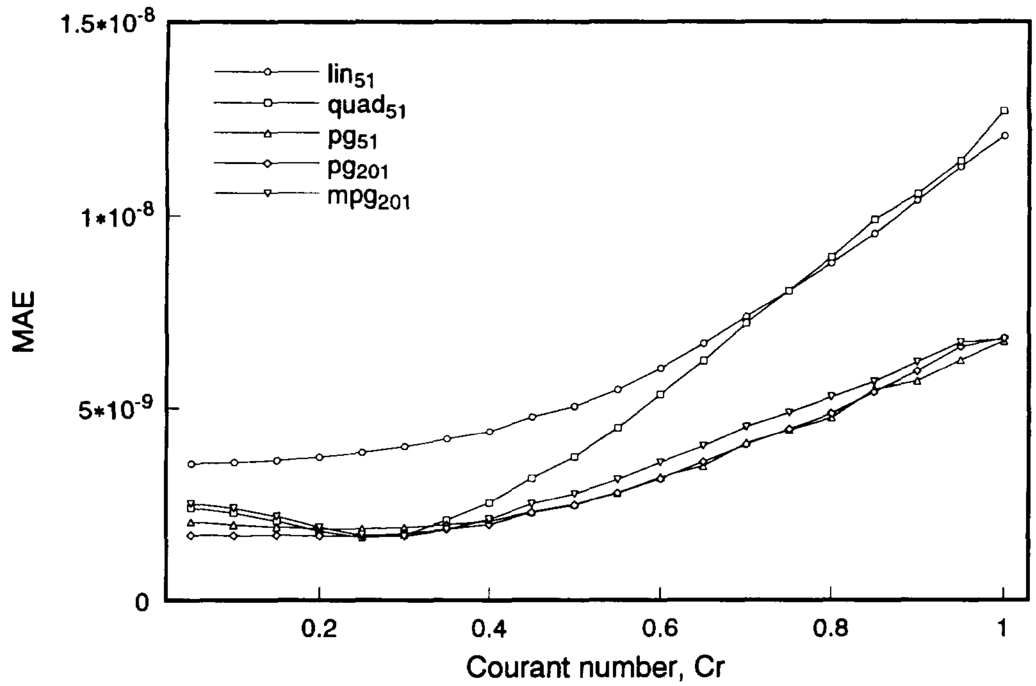

Fig. 12. MAE as a function of model formulation, described in Table 4 (Table 1, case 6).

increased discretization for α_c, α_m, and β_m. Based upon this observation, simulations were performed to evaluate solution errors as a function of PG parameter values and Cr. Case 6 in Table 1 summarizes simulation parameters for results shown in Figures 9–13, while Table 4 summarizes model formulations investigated.

Figure 9 shows that the MSE-h is less for the PG method than for the standard quadratic method for all discretizations. The reduction in error is a maximum for $Cr = 1$, with a 65% reduction observed for the tailored PG run compared to a linear FEM solution. Figure 9 also shows comparisons for MSE-h as a function of PG parameters used. The lowest errors were achieved for optimal parameters based upon the number of nodes in the system (51). However, using optimal PG parameters from a 201-node case for a 51-node system increased the solution errors only slightly. This is significant because it reduces the functional dependence of the optimal PG parameters to just one variable, Cr. It should be noted that for a very small number of nodes ($n_n < 20$), the difference between the optimal and approximate PG solu-

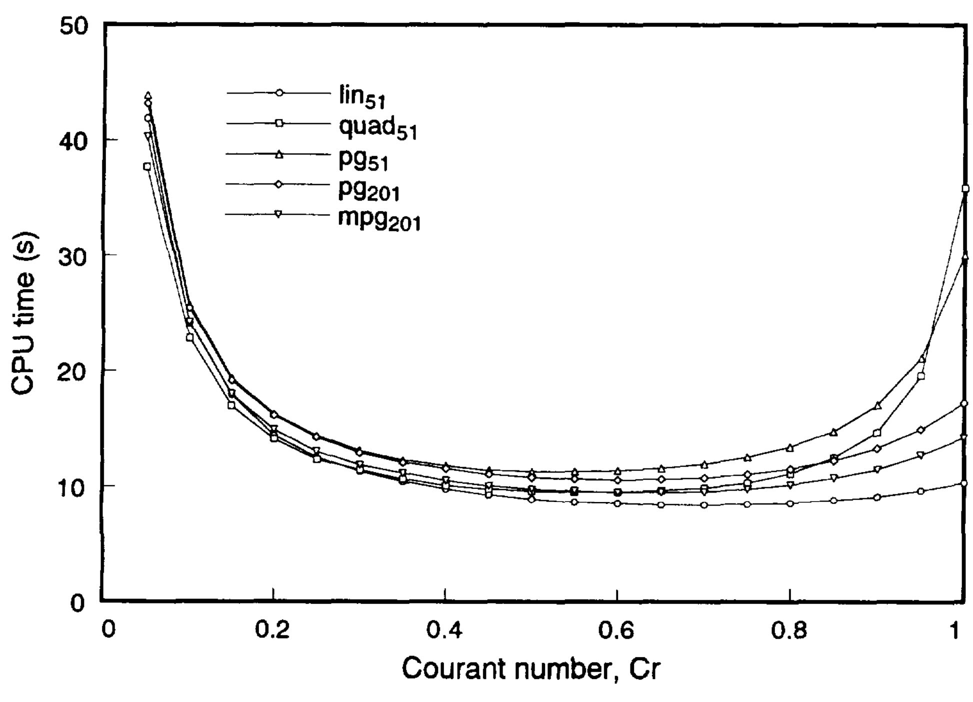

Fig. 13. CPU times as a function of model formulation, described in Table 4 (Table 1, case 6).

TABLE 4. Model Formulation Summary

Case	Method	Optimal Parameters
lin_{51}	Linear Bubnov-Galerkin FEM	...
$quad_{51}$	Quadratic Bubnov-Galerkin FEM	...
pg_{51}	Quadratic Petrov-Galerkin FEM	optimal for $n_n = 51$
pg_{201}	Quadratic Petrov-Galerkin FEM	optimal for $n_n = 201$
mpg_{201}	Modified Quadratic Petrov-Galerkin* FEM	optimal for $n_n = 201$

*Single-parameter PG model ($\alpha_c = \alpha_m = \beta_m = 0$).

tions described above is greater than shown for this 51-node case. Figure 10 shows a similar trend for MSE-q.

The previous observation that α_c, α_m, and β_m approach zero as the number of nodes increases(Figures 5–8) suggests a second level of simplification. This modification is to set all PG parameters to zero except for β_c, giving test functions of the form

$$W_1(\xi) = N_1(\xi) - \beta_c M_4(\xi) \tag{38}$$

$$W_2(\xi) = N_2(\xi) \tag{39}$$

$$W_3(\xi) = N_3(\xi) - \beta_c M_4(\xi) \tag{40}$$

Use of these functions reduces the computational effort compared to the full PG method, while still increasing the accuracy and rate of convergence of the solution over the standard quadratic method. Results from this simplification are shown in Figures 9 and 10 by the run noted as mpg_{201}.

The trends noted above for MSE are consistent with results obtained for other measures of error as well. ME and MAE errors are shown in Figures 11 and 12, respectively. All methods are mass conserving, so mass balance error was negligible for all problems analyzed in this work, therefore not a good measure of solution accuracy.

CPU timing results are shown in Figure 13 for a 51-node system and a simulation time needed to reach a steady state condition. The CPU times are dependent upon the number of time steps taken to approach steady state conditions (i.e., Cr) and the number of iterations needed to converge at each time step. For $Cr < 0.8$, the standard quadratic model (quad) required the least CPU time. However, the CPU time for the quadratic model increased rapidly for $Cr > 0.8$. A similar trend in CPU time was observed for the optimal PG simulations (pg_{51}) as a function of $Cr > 0.8$. The lowest CPU time for all methods occurred for $Cr \approx 0.60$. In view of the error results shown in Figures 9 to 12, this suggests efficient solutions can be obtained using the PG method in terms of both CPU time and solution error at $Cr = 0.6$.

7. CONCLUSIONS

A quadratic Petrov-Galerkin (PG) solution to the kinematic wave overland flow equations was developed and compared to standard linear and quadratic Bubnov-Galerkin finite element solutions and an analytical solution derived from the method of characteristics. Model results were investigated for both water depth profiles (h based) and outflow hydrographs (q based). The PG method required the determination of four parameters, which were evaluated using a Levenberg-Marquardt method. The PG method decreased the mean sum of square error by about 65% compared to a conventional Bubnov-Galerkin linear finite element approximation for a Courant number (Cr) of 1. Encouraging results were also found for shock-type problems, which result from variations in surface slope or roughness. The four PG parameters in the formulation depended strongly upon the Cr and weakly upon the number of nodes (n_n) in the system. A reasonable approximation to the optimal solution was achieved using parameters based upon a fixed number of nodes ($n_n = 201$). Good solutions were also achieved using a single-parameter simplification of the general PG model. Minimum CPU times were achieved for $Cr \approx 0.6$ for all formulations investigated.

*Acknowledgments.*The work upon which this paper is based was supported in part by grants from the U.S. Department of Agriculture Soil Conservation Service, the U.S. Environmental Protection Agency, and the North Carolina Water Resources Research Institute. R.M.C. expresses appreciation for a fellowship from the Instituto Nacional de Investigaciones Agrarias (INIA) of Spain and the U.S. Department of Agriculture. This work was substantially improved by contributions from two anonymous peer reviewers.

REFERENCES

Allen, M. B., I. Herrera, and G. F. Pinder, *Numerical Modeling in Science and Engineering*, Wiley Interscience, New York, 1988.

Amein, M., An implicit method for numerical flood routing, *Water Resour. Res.*, *4*(4), 719–726, 1968.

Amein, M., and C. S. Fang, Implicit flood routing in natural channels, *J. Hydraul. Div. Am. Soc. Civ. Eng.*, *96*(HY12), 2481–2500, 1970.

Bedient, B. P., and W. C. Huber, *Hydrology and Floodplain Analysis*, Addison-Wesley, Reading, Mass., 1988.

Blandford, G. E., and M. Meadows, Finite element simulation of non-linear kinematic surface runoff, *J. Hydrol.*, *119*, 335–356, 1990.

Borah, D. K., S. N. Prasad, and C. V. Alonso, Kinematic wave routing incorporating shock fitting, *Water Resour. Res.*, *16*(3), 529–541, 1980.

Brakensiek, D. L., Kinematic flood routing, *Trans. ASAE*, *10*(3), 340–343, 1967.

Bras, L. R., *Hydrology: An Introduction to Hydrological Science*, Addison-Wesley, Reading, Mass., 1990.

Cantekin, M. E., and J. J. Westerink, Non-diffusive $N + 2$ degree Petrov-Galerkin methods for two-dimensional transient transport computations, *Int. J. Numer. Methods Eng.*, *30*, 397–418, 1990.

Cornew, F. H., and C. T. Miller, An adaptive Petrov-Galerkin finite element method for approximating advective-dispersive-reaction equations, in *Computational Methods in Subsurface Hydrology*, edited by G. Gambolati, A. Rinaldo, C. A. Brebbia, W. G. Gray, and G. F. Pinder, pp. 437–442, Springer-Verlag, New York, 1990.

Crawford, N. H., and R. K. Linsley, Digital simulation in hydrology: Stanford Watershed Model IV, *Tech. Rep. 39*, Dep. of Civ. Eng., Stanford Univ., Stanford, Calif., 1966.

Cundy, T. W., and S. W. Tento, Solution to the kinematic wave approach to overland flow routing with rainfall excess given by Philip's equation, *Water Resour. Res.*, *21*(8), 1132–1140, 1985.

Eagleson, P. S., *Dynamic Hydrology*, McGraw-Hill, New York, 1970.

Eggert, K. G., Upstream calculation of characteristics for kinematic wave routing, *J. Hydraul. Eng.*, *113*(6), 743–752, 1987.
Garbow, B. S., K. E. Hillstrom, and J. J. More, MINPACK Project, report, Argonne Natl. Lab., Argonne, Ill., March 1980.
Goodrich, D. C., D. A. Woolhiser, and T. O. Keefer, Kinematic routing using finite elements on a triangular irregular network, *Water Resour. Res.*, *27*(6), 995–1003, 1991.
Harley, B. M., F. E. Perkins, and P. S. Eagleson, A modular distributed model of catchment dynamics, *Hydrodyn. Rep.* 133, Mass. Inst. of Technol., Cambridge, 1970.
Heinrich, J. C., and O. C. Zienkiewicz, Quadratic finite element schemes for two-dimensional convective transport problems, *Int. J. Numer. Methods Eng.*, *11*, 131–143, 1977.
Henderson, F. M., *Open Channel Flow*, pp. 125–164 and 285–398, Macmillan, New York, 1966.
Henderson, F. M., and R. A. Wooding, Overland flow and groundwater flow from a steady rainfall of finite duration, *J. Geophys. Res.*, *69*(8), 1531–1540, 1964.
Hromadka, T. V., II, and J. J. DeVries, Kinematic wave routing and computational error, *J. Hydraul. Eng.*, *114*(2), 207–217, 1988.
Hughes, T. J. R., A simple scheme for developing upwind finite elements, *Int. J. Numer. Methods Eng.*, *12*, 1359–1365, 1978.
Hunt, B., A perturbation solution of the flood routing problem, *J Hydraul. Res.*, *25*(3), 215–234, 1987.
Huyakorn, P. S., and G. F. Pinder, *Computational Methods in Subsurface Flow*, Academic, San Diego, Calif., 1983.
Iwagaki, Y., Fundamental studies on runoff analysis by characteristics, *Bull. Disaster Prev. Res. Inst. Kyoto Univ.*, *10*, 1955.
Izzard, C. F., Hydraulics of runoff from developed surfaces, *Proc. Annu. Meet. Highw. Res. Board*, *26*, 126–146, 1946.
Judah, O. M., Simulation of runoff hydrographs from natural watersheds by finite element method, Ph.D. thesis, Va. Polytechnic Inst. and State Univ., Blacksburg, Va., 1972.
Kibler, D. F., and D. A. Woolhiser, Mathematical properties of the kinematic cascade, *J. Hydrol.*, *15*, 131–147, 1972.
Lane, L. J., G. R. Foster, and A. D. Nicks, Use of fundamental erosion mechanics in erosion prediction, paper 87-2540 presented at the 1987 Winter Meeting of the American Society of Agricultural Engineers, Chicago, Ill., 1987.
Li, R. M., D. B. Simons, and M. A. Stevens, Nonlinear kinematic wave approximation for water routing, *Water Resour. Res.*, *11*(2), 245–252, 1975.
Liggett, J. A., and D. A. Woolhiser, Difference solutions of the shallow water equation, *J. Eng. Mech. Div. Am. Soc. Civ. Eng.*, *93*(EM2), 39–71, 1967.
Lighthill, M. J., and C. B. Whitham, On kinematic waves: Flood movement in long rivers, *Proc. R. Soc. London, Ser. A*, *229*, 281–316, 1955.
Mayer, A. S., and C. T. Miller, A compositional model for simulating multiphase flow, transport and mass transfer in groundwater systems, in *Computational Methods in Subsurface Hydrology*, edited by G. Gambolati, A. Rinaldo, C. A. Brebbia, W. G. Gray, and G. F. Pinder, pp. 217–222, Springer-Verlag, New York, 1990.
Miller, C. T., and F. H. Cornew, A Petrov-Galerkin method for resolving advective-dominated transport, in *Computational Methods in Water Resoures IX*, vol. 1, *Numerical Methods in Water Resources*, edited by T. F. Russell, R. E. Ewing, C. A. Brebbia, W. G. Gray, and G. F. Pinder, pp. 157–164, Elsevier, New York, 1992.
Mohtar, R. H., B. E. Vieux, and L. J. Segerlind, Control volume finite element solution for surface flow equations, paper 90-2631 presented at the 1990 Winter Meeting of the American Society of Agricultural Engineers, Chicago, Ill., Dec. 1990.
Parlange, J.-Y., C. W. Rose, and G. C. Sander, Kinematic flow approximation of runoff on a plane: An exact analytical solution, *J. Hydrol.*, *52*, 171–176, 1981.
Ponce, V. M., The kinematic wave controversy, *J. Hydraul. Eng.*, *117*(4), 511–525, 1991.
Price, R. K., Comparison of four numerical methods for flood routing, *J. Hydraul. Div. Am. Soc. Civ. Eng.*, *100*(HY7), 879–899, 1974.
Richards, L. A., Capillary conduction of liquids in porous mediums, *Physics*, *1*, 318–333, 1931.
Ross, R. B., Finite element simulation of overland flow and channel flow, *Trans. ASAE*, *20*(4), 705–712, 1977.
Ross, R. B., D. N. Contractor, and V. O. Shanholtz, A finite element model of overland and channel flow for assessing the hydrologic impact of land-use change, *J. Hydrol.*, *41*, 11–30, 1979.
Sander, G. C., J.-Y. Parlange, W. L. Hogarth, C. W. Rose, and R. Haverkamp, Kinematic flow approximation to runoff on a plane: Solution for infiltration rate exceeding rainfall rate, *J. Hydrol.*, *113*, 193–206, 1990.
Schmid, B. H., On overland flow modelling: Can rainfall excess be treated as independent of flow depth?, *J. Hydrol.*, *107*, 1–8, 1989.
Sherman, B., and V. J. Singh, A distributed converging overland flow model, 1, Mathematical solutions, *Water Resour. Res.*, *12*(5), 889–896, 1976.
Singh, V. J., Hybrid formulation of kinematic wave models of watershed runoff, *J. Hydrol.*, *27*, 33–50, 1975.
Singh, V. J., A distributed converging overland flow model, 3, Application to natural watersheds, *Water Resour. Res.*, *12*(5), 902–907, 1976.
Skaggs, R. W., L. E. Huggins, E. J. Monke, and G. R. Foster, Experimental evaluation of infiltration equations, *Trans. ASAE*, *12*(6), 822–828, 1969.
Stoker, J. J., Numerical solution of flood prediction and river regulation problems, I, Derivation of basic theory and formulation of numerical methods of attack, *Rep. IMM-200*, Inst. of Math. Sci., New York Univ., New York, 1953.
Taylor, C., A computer simulation of direct run-off, in *Finite Elements in Water Resources*, edited by W. G. Gray, G. F. Pinder, and C. A. Brebbia, pp. 4.149–4.163, Pentech, London, 1976.
Viessman, W., Jr., J. W. Knapp, G. L. Lewis, and T. E. Harbaugh, *Introduction to Hydrology*, 2nd ed., Harper Collins, New York, 1977.
Vieux, B. E., and L. J. Segerlind, Finite element solution accuracy of an infiltrating channel, paper presented at 7th International Conference on Finite Element Methods in Flow Problems, Univ. of Ala., Huntsville, 1989.
Vieux, B. E., V. F. Bralts, L. J. Segerlind, and R. B. Wallace, Finite element watershed modeling: One-dimensional elements, *J. Water Resour. Plan. Manage. Div Am. Soc. Civ. Eng.*, *116*(6), 803–819, 1990.
Wait, R., and A. R. Mitchell, *Finite Element Analysis and Applications*, John Wiley, New York, 1985.
Westerink, J. J., and D. Shea, Consistent higher degree Petrov-Galerkin methods for the solution of the transient convection-diffusion equation, *Int. J. Numer. Methods Eng.*, *28*, 1077–1101, 1989.
Wooding, R. A., A hydraulic model for the catchment-stream problem, II, Numerical solutions, *J. Hydrol.*, *3*, 268–282, 1965.
Woods, R. A., and R. P. Ibbitt, Analytical solution for kinematic flow over an infiltrating plane, paper presented at the International Symposium on Modeling Agricultural, Forest and Rangeland Hydrology, Am. Soc. of Agric. Eng., Chicago, Ill., 1988.
Woolhiser, D. A., Overland flow on a converging surface, *Trans. ASAE*, *12*(4), 460–462, 1969.
Woolhiser, D. A., Simulation of unsteady overland flow, in *Unsteady Flow in Open Channels*, vol. II, edited by K. Mahmood and V. Yevjevich, pp. 485–508, Water Resource Publications, Fort Collins, Colo., 1975.
Woolhiser, D. A., and J. A. Liggett, Unsteady, one-dimensional flow over a plane: The rising hydrograph, *Water Resour. Res.*, *3*(3), 753–771, 1967.
Zhang, W., and T. W. Cundy, Modeling of two-dimensional overland flow, *Water Resour. Res.*, *25*(9), 2019–2035, 1989.
Zienkiewicz, O. C., *The Finite Element Method*, 3rd ed., McGraw-Hill, New York, 1977.

C. T. Miller, CB 7400, 114 Rosenau Hall, Department of Environmental Sciences and Engineering, The University of North Carolina, Chapel Hill, NC 27599-7400.

R. Muñoz-Carpena and J. E. Parsons, Biological and Agricultural Engineering, North Carolina State University, Raleigh, NC 27695-7625.

(Received September 16, 1992;
revised February 16, 1993;
accepted March 8, 1993.)